Mycobacterium tuberculosis persistence mutants identified by screening in isoniazid-treated mice

Neeraj Dhar[1] and John D. McKinney

Global Health Institute, Swiss Federal Institute of Technology (EPFL), 1015 Lausanne, Switzerland

Edited by Ralph R. Isberg, Tufts University School of Medicine, Boston, MA, and approved May 28, 2010 (received for review March 15, 2010)

Tuberculosis (TB) is notoriously difficult to cure, requiring administration of multiple antibiotics for 6 mo or longer. Conventional anti-TB drugs inhibit biosynthetic processes involved in cell growth and division, such as DNA replication, RNA transcription, protein translation, and cell wall biogenesis. Although highly effective against bacteria cultured in vitro under optimal growth conditions, these antibiotics are less effective against bacteria grown in vivo in the tissues of a mammalian host. The factors that contribute to the antibiotic tolerance of bacteria grown in vivo are unknown, although altered metabolism and sluggish growth are hypothesized to play a role. To address this question, we identified mutations in *Mycobacterium tuberculosis* that impaired or enhanced persistence in mice treated with isoniazid (INH), a front-line anti-TB drug. Disruption of *cydC*, encoding a putative ATP-binding cassette transporter subunit, accelerated bacterial clearance in INH-treated mice without affecting growth or survival in untreated mice. Conversely, transposon insertions within the *rv0096–rv0101* gene cluster attenuated bacterial growth and survival in untreated mice but paradoxically prevented INH-mediated killing of bacteria in treated mice. These contrasting phenotypes were dependent on the interaction of the bacteria with the tissue environment because both mutants responded normally to INH when grown in macrophages ex vivo or in axenic cultures in vitro. Our findings have important implications because persistence-impairing mutations would be missed by conventional genetic screens to identify candidate drug targets. Conversely, persistence-enhancing mutations would be missed by standard diagnostic methods, which are performed on bacteria grown in vitro, to detect drug resistance.

chemotherapy | drug tolerance | host environment

Tuberculosis (TB) has been a treatable disease for more than half a century, yet TB eradication remains a distant and possibly unachievable goal barring the introduction of more effective control strategies (1). A formidable obstacle to successful treatment of TB is the requirement for frequent administration of multiple drugs for 6 mo or longer (2). Unless drug administration is closely supervised, the majority of patients will not adhere to such a protracted therapeutical regimen (2). Consequently, patient nonadherence is responsible for high rates of treatment failure, relapse, and emergent drug resistance (3). To reduce treatment costs and improve patient adherence, there is an urgent need for more effective anti-TB drugs to shorten the treatment time (2, 4).

Conventional anti-TB drugs target biosynthetic processes involved in cell growth, including RNA transcription [rifampicin (RIF)], protein translation (streptomycin), and cell wall biogenesis [isoniazid (INH)]. Although these drugs rapidly kill *Mycobacterium tuberculosis* grown in vitro, they are less active against bacteria grown in vivo in mammalian hosts (4, 5). In the mouse model of TB, infection progresses through a brief acute phase, when bacteria replicate exponentially in the lungs, to a protracted chronic phase, when growth slows and bacterial numbers are stabilized by the immune response (6–8). Anti-TB drugs like INH display good bactericidal activity in acutely infected mice, but chronic infection is more refractory (9). The physiological basis of *M. tuberculosis* persistence in drug-treated hosts is unknown, although sluggish bacterial metabolism and growth are thought to contribute (4).

Herein, we identify mutations that impaired or enhanced *M. tuberculosis* persistence in INH-treated mice. These phenotypes were environment-specific, inasmuch as neither class of mutations altered the persistence of INH-treated populations of bacteria grown in murine macrophages ex vivo or in axenic cultures in vitro. These findings suggest that screening in antibiotic-treated animals has the potential to reveal persistence targets that would be missed by conventional screens. This approach could also be useful for target invalidation, based on the knowledge that disruption of the corresponding gene enhances persistence in antibiotic-treated animals. Ideally, any newly developed drug should synergize with existing therapeutical agents; at the very least, a newly developed drug should not interfere with them. The screening approach described herein could be a strategy for achieving both objectives.

Results

***M. tuberculosis* Persistence Mutants.** We designed a genetic screen to identify mutations that impair or enhance *M. tuberculosis* persistence in a murine chemotherapy model (Fig. 1*A*). We focused on INH because it is a cornerstone of anti-TB therapy and because *M. tuberculosis* persistence in INH-treated mice (9) and TB patients (10) is well documented. Also, INH is particularly sensitive to the stage of infection, exhibiting much better activity in acutely infected mice than in chronically infected mice (9).

C57BL/6 mice were infected i.v. with pools of *M. tuberculosis* mutants generated by signature-tagged transposon mutagenesis (Fig. 1*A*). In the i.v. infection model, bacteria replicate exponentially in the lungs for the first 2 wk postinfection; thereafter, bacterial numbers remain relatively stable for several months (6–8). From 4 wk onward, half of the mice were treated with INH. Lungs were harvested from untreated and INH-treated mice at 6 or 12 wk, and the recovered signature tags were quantified (*Materials and Methods*). We chose these time points for analysis to distinguish the impact of mutations on bacterial persistence at early (6 wk) and later (12 wk) stages of INH therapy.

We screened a total of 12 pools comprising 576 signature-tagged transposon mutants. Three distinct classes of mutants were identified, reflecting impaired, enhanced, or normal persistence in INH-treated mice (Fig. 1*B*). As expected, most of the mutants showed normal representation in pools recovered from INH-treated mice (e.g., Fig. 1*C*). Persistence-impaired mutants were underrepresented in INH-treated mice as compared with untreated mice (e.g., Fig. 1*D*). Conversely, persistence-enhanced mutants were overrepresented in INH-treated mice as compared with untreated mice. Interestingly, some of the mutants in this class were also attenuated for growth/survival in untreated mice (e.g., Fig. 1*E*). Persistence enhancement was not, however,

Author contributions: N.D. and J.D.M. designed research; N.D. performed research; N.D. and J.D.M. analyzed data; and N.D. and J.D.M. wrote the paper.

The authors declare no conflict of interest.

Freely available online through the PNAS open access option.

This article is a PNAS Direct Submission.

[1]To whom correspondence should be addressed. E-mail: neeraj.dhar@epfl.ch.

This article contains supporting information online at www.pnas.org/lookup/suppl/doi:10.1073/pnas.1003219107/-/DCSupplemental.

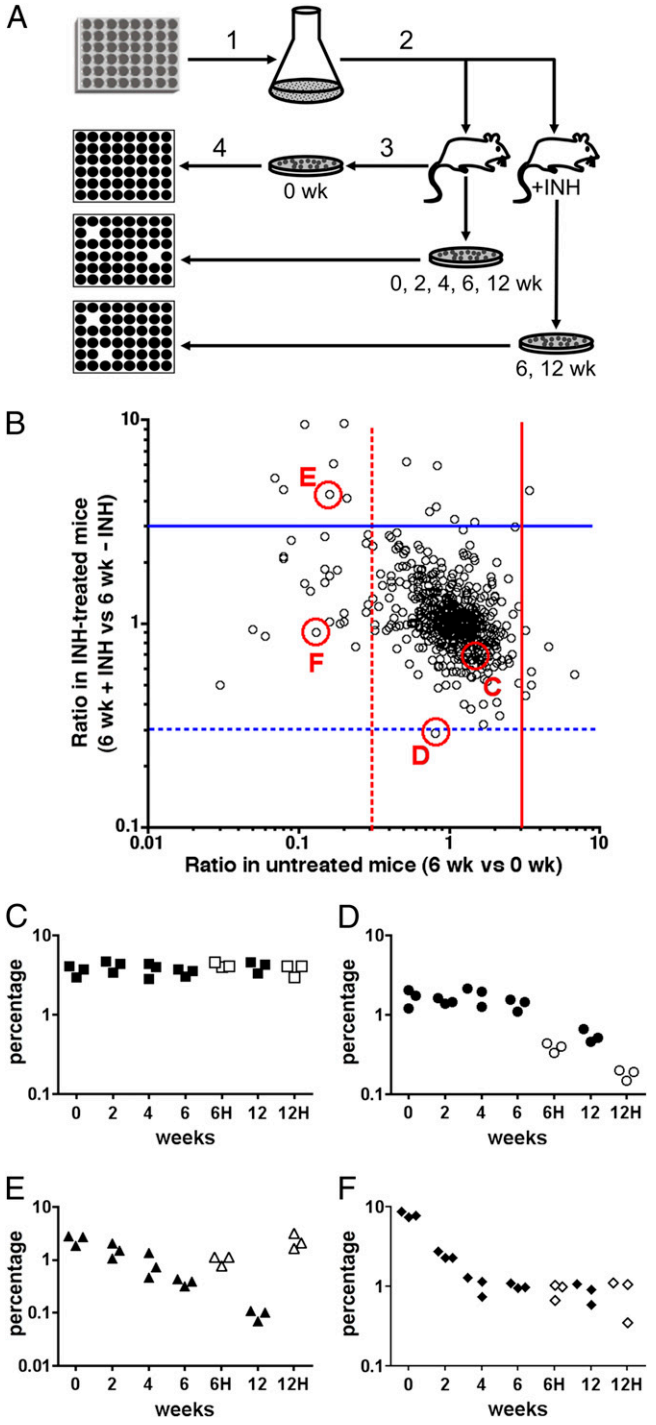

Fig. 1. Comparative screening of *M. tuberculosis* mutants in untreated vs. INH-treated mice. (*A*) Screening strategy to identify *M. tuberculosis* mutants with impaired or enhanced persistence in INH-treated mice. (1) Individual signature-tagged mutants are arrayed in 48-well microplates and pooled. (2) C57BL/6 mice are inoculated with pools of mutants and left untreated or treated with INH from 4 wk postinfection onward. (3) Bacteria are recovered by plate culture of lung homogenates. (4) Signature tags from untreated and INH-treated mice are radiolabeled and measured by membrane hybridization and PhosphorImager analysis. (*B*) Correlation plot of 576 mutants screened in untreated vs. INH-treated mice. Each symbol represents one tag, expressed as a percentage of the total hybridization signal for all 48 tags in the same pool. The *x* axis plots the ratio of each tag's representation in untreated mice at 6 vs. 0 wk. Mutants to the left of the vertical dashed line are attenuated for growth/survival in untreated mice. The *y* axis plots the ratio of each tag's representation in INH-treated mice vs. untreated mice at 6 wk. Mutants below the horizontal dashed line are persistence-impaired, and mutants above the horizontal solid line are persistence-enhanced. Arbitrary values of 0.33 and 3.0 were chosen as cutoffs for selection of mutants for further analysis, indicated by red circles and letters. Tag hybridization signals are shown for mutants with the following phenotypes: normal (e.g., WT) in untreated and INH-treated mice (*C*); persistence-impaired in INH-treated mice (*D*); persistence-enhanced in INH-treated mice but growth/survival-attenuated in untreated mice (*E*); and growth/survival-attenuated in untreated mice (*F*). Each symbol represents the tag from one mouse. H, INH.

a phenotype shared by all mutants that displayed growth/survival defects in untreated mice (e.g., Fig. 1*F*).

Historically, signature-tagged mutagenesis has been used to identify mutants with growth or survival defects in untreated animals (11–13). Our screening scheme was complicated by the fact that the entire population of pooled mutants was progressively reduced by INH therapy, which could lead to artifactual underrepresentation or overrepresentation of individual mutants. To confirm the results of our screen, we selected for further analysis one representative mutant of each class representing normal (Fig. 1*C*), impaired (Fig. 1*D*), or enhanced (Fig. 1*E*) persistence in INH-treated mice. The site of transposon insertion in the chromosome of each mutant was identified as described in *Materials and Methods*.

***cydC* Disruption Impairs *M. tuberculosis* Persistence.** A persistence-impaired *M. tuberculosis* mutant (Fig. 1*D*) contained a transposon insertion in the *rv1620c* (*cydC*) ORF. *cydC* is the last ORF in an annotated four-gene cluster (*cydABDC*) (Fig. S1). In *Escherichia coli*, *cydA* and *cydB* encode subunits I and II of the cytochrome *bd*-quinol oxidase required for microaerobic respiration; *cydD* and *cyd*C encode an ATP-binding cassette (ABC) transporter required for cytochrome *bd* assembly (14). In *M. tuberculosis*, expression of *cydABDC* is up-regulated by exposure to hypoxia or nitric oxide in vitro and during the chronic phase of infection in mice (15).

We confirmed the phenotypes of the *cydC*::Tn mutant by infecting C57BL/6 mice with WT or *cydC*::Tn bacteria and measuring cfus in mice that were untreated or treated with INH from 4 wk postinfection onward (Fig. 2). In untreated mice, the WT (Fig. 2 *A* and *B*) and *cydC*::Tn (Fig. 2 *C* and *D*) strains showed similar kinetics of growth and survival in the lungs (Fig. 2 *A* and *C*) and spleens (Fig. 2 *B* and *D*). Previously, another group reported that disruption of *cydC* impaired survival of *M. tuberculosis* in untreated mice (15); we do not know the reason for the discrepancy between their results and ours. It is possible that the use of different *M. tuberculosis* strain backgrounds in the two studies (H37Rv in theirs, Erdman in ours) might account for the difference. In the organs of INH-treated mice, persistence of the *cydC*::Tn mutant (Fig. 2 *C* and *D*) was markedly impaired as compared with the WT control strain (Fig. 2 *A* and *B*). After 8 wk of INH therapy (12 wk postinfection), persistence of the WT and *cydC*::Tn strains was significantly different in the lungs (0.13% vs. 0.004%; $P < 0.005$) and spleens (0.29% vs. 0.005%; $P < 0.000005$) (Tables S1 and S2). We conclude that *M. tuberculosis* persistence in INH-treated mice is dependent on the putative ABC transporter encoded by *cydDC*.

Complementation Analysis. Complementation of the *cydC*::Tn mutant with a single-copy integrating plasmid containing the intact *cydC* gene reversed the persistence defect in the spleens of INH-treated mice (Fig. S2*B* and Table S2). Complementation also restored persistence of the *cydC*::Tn mutant in the lungs of INH-treated mice, although not to WT levels (Fig. S2*A* and Table S1). Failure to achieve complete complementation might be attributable to unbalanced expression of the CydC protein from the heterologous *hsp60* promoter in relation to other gene products of the *cydABDC* locus, particularly CydD, with which CydC is predicted to form heterodimers. It is noteworthy that impaired persistence of the *cydC*::Tn mutant was specific to established infection because

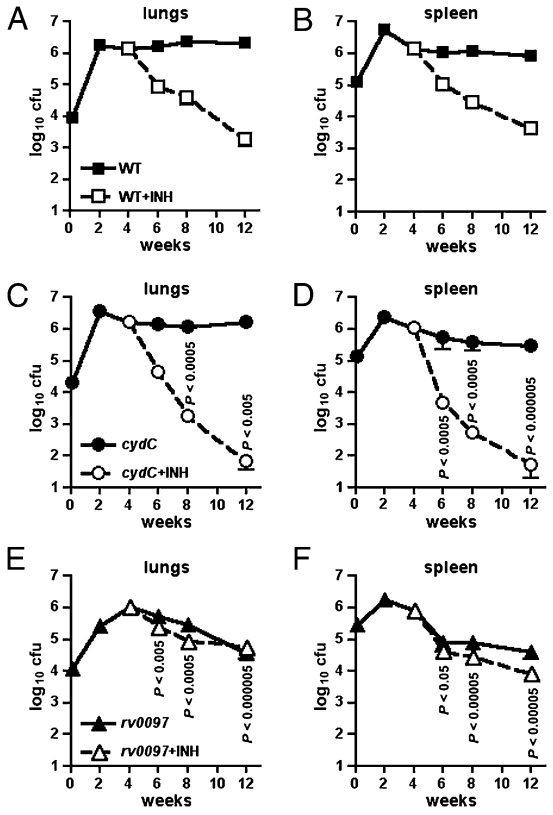

Fig. 2. Persistence of *cydC*::Tn and 5′Tn::*rv0097* bacteria in INH-treated mice. C57BL/6 mice were infected i.v. with ~1 × 10^6 cfus of WT (*A* and *B*), *cydC*::Tn (*C* and *D*), or 5′Tn::*rv0097* (*E* and *F*) bacteria. From 4 wk postinfection onward, groups of mice were left untreated (filled symbols) or were treated with INH (empty symbols). Bacterial cfus were measured in the lungs (*A*, *C*, and *E*) and spleens (*B*, *D*, and *F*) at the indicated time points. Symbols represent mean ± SEM ($n = 4$). Results are representative of three experiments. Tukey's honestly significant difference test was used to compare the effectiveness of drug therapy (untreated vs. treated mice) against WT vs. mutant bacteria. *P* values are indicated for each time point where $P < 0.05$.

WT and *cydC*::Tn bacteria were killed with the same kinetics when INH therapy was initiated at 24 h postinfection (Fig. S2 *C* and *D*).

Drug Specificity. To determine whether the persistence defect of the *M. tuberculosis cydC*::Tn mutant was drug-specific, chronically infected mice were treated with RIF or pyrazinamide (PZA) from 4 wk postinfection onward. The impact of *cydC* disruption on drug-mediated killing was INH-specific because WT (Fig. S3 *C* and *D*) and *cydC*::Tn (Fig. S3 *E* and *F*) bacteria were cleared with similar kinetics in mice receiving RIF (Fig. S3 *C* and *E*) or PZA (Fig. S3 *D* and *F*) monotherapy. In clinical practice, INH is administered in combination with other antimicrobials, notably RIF. As expected, the combination of INH + RIF was more effective than either drug alone, and the accelerated clearance of *cydC*::Tn mutant bacteria was preserved in mice treated with INH + RIF (Fig. S3 *A* and *B*). Thus, although *cydC* deficiency did not impair *M. tuberculosis* persistence in RIF-treated mice, RIF did not mask the enhanced killing of *cydC*::Tn bacteria by INH.

***rv0096–rv0101* Disruption Enhances *M. tuberculosis* Persistence.** A persistence-enhanced *M. tuberculosis* mutant (Fig. 1*E*) contained a transposon insertion 11 base pairs upstream of the *rv0097* ORF, which encodes a putative oxidoreductase of the *tfdA* dioxygenase family (Fig. S1). *rv0097* is part of an operon, *rv0096–rv0101* (16), that is required for survival of *M. tuberculosis* in mouse macrophages (17). Recently, *rv0098* was identified as a type III thioesterase, and it was hypothesized that this enzyme hydrolyzes fatty acyl-CoA substrates to generate free C_{16}–C_{18} fatty acids, which are used in the synthesis of lipopeptides (18). Other genes within the operon encode a PPE protein family member (Rv0096), a fatty acid AMP ligase (Rv0099), an acyl carrier protein (Rv0100), and a nonribosomal peptide synthase (Rv0101).

We confirmed the phenotypes of the 5′Tn::*rv0097* mutant by infecting C57BL/6 mice with WT or 5′Tn::*rv0097* bacteria and measuring cfus in the organs of mice that were untreated or treated with INH from 4 wk postinfection onward (Fig. 2). Consistent with the results of the screen, the 5′Tn::*rv0097* mutant was growth-attenuated in the lungs (Fig. 2*E*) and spleens (Fig. 2*F*) of untreated mice as compared with WT bacteria (Fig. 2 *A* and *B*). We also confirmed that the 5′Tn::*rv0097* mutant was refractory to INH-mediated killing in the lungs (Fig. 2*E*) and spleens (Fig. 2*F*), inasmuch as the bacterial cfus obtained from untreated and INH-treated mice were not significantly different (Tables S1 and S2). In contrast to the effects of *cydC* disruption, which were INH-specific, the 5′Tn::*rv0097* mutant was also refractory to killing by RIF (Fig. S3*G* and Table S1) and PZA (Fig. S3*H* and Table S1). To rule out the possibility that enhanced persistence was attributable to increased frequency of drug-resistance mutations, organ homogenates from the INH-treated mice were plated on solid medium containing 0.2 μg/mL INH. The fraction of INH-resistant colonies was found to be similar for the WT and 5′Tn::*rv0097* strains, ~0.06% in both cases.

We conclude that mutations that impair bacterial fitness in untreated mice can, in some cases, paradoxically enhance persistence in drug-treated mice. The transposon insertion in the 5′Tn::*rv0097* mutant reduced the expression of all the genes in the *rv0096–rv0101* operon (Table S3). It is unclear which gene(s) is responsible for the phenotypes observed in untreated and drug-treated mice, and the number of genes involved ($n = 6$) makes complementation analysis impracticable. However, by screening in INH-treated mice, we identified an independent mutant with a transposon insertion in the *rv0096* ORF. The *rv0096*::Tn mutant exhibited the same phenotypes as the 5′Tn::*rv0097* mutant (Fig. S4), which supports the conclusion that the product(s) of one or more genes in the *rv0096–rv0101* cluster promotes normal growth and survival in untreated mice yet interferes with persistence in drug-treated mice.

Growth Attenuation and Persistence Enhancement Are Dissociable Phenotypes. Drugs that target cell wall biogenesis, such as INH, are more effective against fast-growing than slow-growing or nongrowing bacteria (4, 5). The phenotypes of the *M. tuberculosis* 5′Tn::*rv0097* mutant suggested the possibility that mutations that impair bacterial growth in untreated mice might also, as a consequence of growth impairment, promote persistence in INH-treated mice. Inconsistent with this interpretation, we identified other mutations that attenuated bacterial growth in untreated mice without altering the kinetics of bacterial death in INH-treated mice (Fig. 1*B*).

To confirm these preliminary observations, we selected one such mutant (Fig. 1*F*) for further analysis. This mutant contained a transposon insertion within a transcriptional promoter upstream of *rv2930* (*fadD26*) (Fig. S1). In a previous report, it was shown that a transposon insertion at the same site impaired growth of *M. tuberculosis* in the lungs but not in the spleens of untreated mice (12). Consistent with this report, we found that growth of the 5′Tn::*fadD26* mutant was impaired in the lungs (Fig. S5*C*) but not in the spleens (Fig. S5*D*) of untreated mice, as compared with the WT strain (Fig. S5 *A* and *B*). We also confirmed that the kinetics of INH-mediated killing were similar in the organs of mice infected with WT bacteria (Fig. S5 *A* and *B*) or 5′Tn::*fadD26* bacteria (Fig. S5 *C* and *D*). Finally, we confirmed that chromosomal transposon insertions per se did not affect persistence of *M. tuberculosis* in INH-treated mice by using a strain with a neutral transposon insertion (Fig. 1*C*) in the *esxD*

gene, which did not affect growth or survival in untreated or treated mice (Fig. S5 *E* and *F*). We conclude that recalcitrance to INH-mediated killing, as exhibited by the 5′Tn::*rv0097* mutant, is a common but not inevitable phenotype of *M. tuberculosis* mutants that are attenuated for growth/survival in vivo.

Role of the in Vivo Environment. When grown in liquid cultures in vitro, WT, *cydC*::Tn, and 5′Tn::*rv0097* bacteria displayed similar rates of exponential phase growth (Fig. 3*A* and Fig. S6*A*) and stationary phase survival (Fig. S7A). The INH minimum inhibitory concentration was the same for the WT, *cydC*::*Tn* mutant, and 5′Tn::*rv0097* mutant strains (0.031 μg/mL). These strains also exhibited similar kinetics of INH-mediated killing in liquid cultures (Fig. 3*B* and Fig. S6*B*), but the emergence of INH-resistant variants after prolonged incubation confounded interpretation of results from long-term experiments. We therefore performed experiments using a combination of INH and ethambutol (EMB) to prevent takeover of the cultures by INH-resistant variants. We found that the rate and extent of killing of WT, *cydC*::Tn, and 5′Tn::*rv0097* bacteria by INH + EMB were similar in exponential phase cultures (Fig. 3*C* and Fig. S6*C*) and in stationary phase cultures (Fig. 3*D* and Fig. S6*D*). We attempted to reproduce the mutant phenotypes observed in mice by subjecting the bacteria to stresses that are thought to mimic the in vivo tissue environment. However, none of the tested conditions uncovered any difference in INH persistence between the WT and mutant strains. This was true even of stresses that induce expression of the *cydABDC* operon (15), such as nitric oxide (Fig. 3*E*) and potassium cyanide (Fig. 3*F*).

We also assessed the activity of INH against bacteria grown in mouse bone marrow-derived macrophages (MBMMs) that were cultured and infected ex vivo. Consistent with the phenotypes observed in untreated mice, the WT (Fig. 3*G* and Fig. S6*E*) and *cydC*::Tn (Fig. 3*H*) bacteria displayed similar growth kinetics in MBMMs, whereas the 5′Tn::*rv0097* strain was impaired for intracellular replication (Fig. S6*F*). However, in contrast to the phenotypes observed in INH-treated mice, INH-mediated killing of intracellular bacteria was similar for the WT (Fig. 3*G* and Fig. S6*E*), *cydC*::Tn (Fig. 3*H*), and 5′Tn::*rv0097* (Fig. S6*F*) strains. This was true even when the bacteria were adapted to the intracellular environment for 24 or 96 h before the addition of INH (Fig. S7 *B* and *C*) or when the macrophages were activated with IFN-γ (Fig. S7 *D*–*F*). We conclude that the persistence-impaired and persistence-enhanced phenotypes of the *cydC*::Tn and 5′Tn::*rv0097* strains, as exhibited in INH-treated mice, are dependent on some aspect of the host–pathogen interaction that is not mimicked by growth of the bacteria in MBMMs ex vivo or in axenic cultures in vitro.

Role of the Host Immune Response. During infection, the physiology of pathogenic bacteria is influenced by the local tissue microenvironments. As infection progresses, the bacteria must further adapt their physiology in response to the complex environmental changes imposed by the host immune response. We hypothesized that immune-mediated environmental changes might contribute to the enhanced killing of *cydC*::Tn bacteria by INH because we did not observe this enhancement when bacteria were grown in vitro, in MBMMs, or in acutely infected (preimmune) mice.

In the mouse model of TB, the cytokine IFN-γ plays a critical role in adaptive immunity by up-regulating expression of the phagosomal guanosine triphosphatase Irgm1/LRG-47 (19, 20) and the inducible nitric oxide synthase (21). We therefore asked whether these host defense mechanisms might be required for enhanced killing of *cydC*::Tn bacteria by INH. C57BL/6, NOS2$^{-/-}$, and Irgm1$^{-/-}$ mice were infected by the respiratory route with ~200 cfus of WT or *cydC*::Tn strains of *M. tuberculosis*. From 2 wk postinfection onward, groups of mice were left untreated or treated with INH. In untreated mice, the WT and *cydC*::Tn strains exhibited similar replication kinetics in the lungs of C57BL/6, NOS2$^{-/-}$, and Irgm1$^{-/-}$ mice (Fig. 4*A*). In INH-treated C57BL/6 mice, the *cydC*::Tn bacteria were cleared more rapidly than WT bacteria (Fig. 4*B*). These observations confirm the results from i.v.-infected mice and demonstrate that the mutant phenotype is independent of the inoculation route. In contrast, enhanced INH-

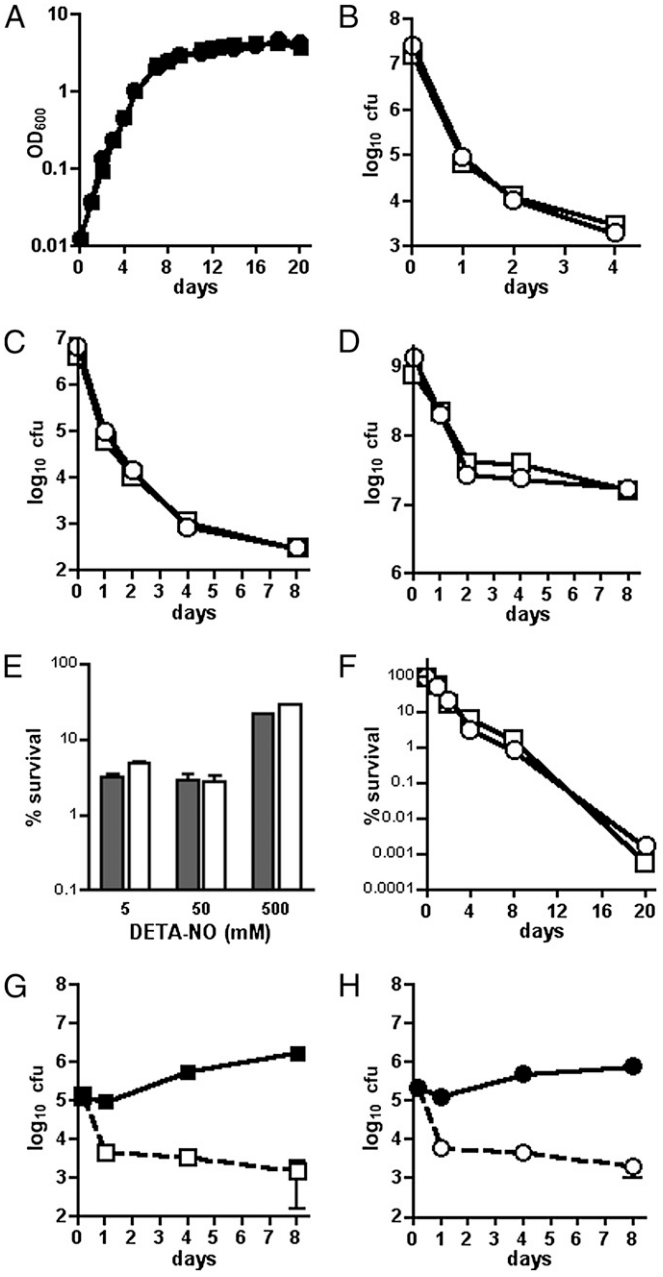

Fig. 3. INH-mediated killing of *cydC*::Tn bacteria grown in vitro or in MBMMs. WT (squares) and *cydC*::Tn (circles) bacteria were grown in 7H9 broth (*A*–*F*) or in MBMMs (*G* and *H*), and OD_{600} or cfus were measured at the indicated time points. (*A*) Bacteria were grown without INH. Bacteria in exponential phase (*B* and *C*) or stationary phase (*D*) were incubated with 1 μg/mL INH (*B*) or with 1 μg/mL INH plus 10 μg/mL EMB (*C* and *D*). Results are representative of four experiments. (*E*) WT (gray bars) and *cydC*::Tn (white bars) bacteria were treated with Diethylenetriamine/nitric oxide adduct (DETA-NO) for 4 h, followed by 1 μg/mL INH for 24 h. Results are representative of two experiments. (*F*) WT (□) and *cydC*::Tn (○) bacteria were treated with 10 μg/mL potassium cyanide (KCN) and 0.2 μg/mL INH. Results are representative of three experiments. WT (*G*) and *cydC*::Tn (*H*) bacteria were grown in MBMMs without (filled symbols) or with (empty symbols) 0.75 μg/mL INH added at 4 h postinfection. Intracellular cfus were measured at the indicated time points. Symbols represent mean ± SEM (n = 3). Results are representative of two experiments.

mediated killing of *cydC*::Tn bacteria was not observed in NOS2$^{-/-}$ mice (Fig. 4*C*) or in Irgm1$^{-/-}$ mice (Fig. 4*D*). Although there was a statistically insignificant trend toward enhanced killing of the *cydC*::Tn mutant in the Irgm1$^{-/-}$ mice, this difference was not observed when the experiment was repeated. We conclude that the enhanced killing of *cydC*::Tn bacteria by INH is dependent on environmental changes imposed by the IFN-γ–mediated immune response.

Discussion

Antimicrobial drug discovery has traditionally focused on cell- or target-based approaches on the assumption that functions essential for bacterial survival under defined conditions in vitro will also be essential in the more complex milieu of infected tissues. This assumption is problematical for several reasons. First, functions that are essential in vitro are not necessarily essential in vivo. For example, glycolysis is required for in vitro growth of *Mycobacterium bovis* on standard media containing carbohydrates as the carbon/energy source, yet this pathway is dispensable for in vivo growth and virulence (22). Likewise, although the methylcitrate cycle is essential for growth of *M. tuberculosis* on fatty acid-containing medium in vitro and in cultured macrophages ex vivo, this pathway is dispensable for growth and virulence in mice (23). Second, and conversely, functions that are essential in vivo are not necessarily essential in vitro. For example, the gluconeogenesis pathway is dispensable for growth of *M. bovis* bacillus Calmette–Guérin on standard medium in vitro, yet this pathway is essential for growth in macrophages and in mice (24). For these reasons, screening for essential functions in vitro is bedeviled by "false-positive" and "false-negative" ascertainment biases.

In light of the disparity between in vitro and in vivo gene essentiality, attention has gradually shifted to target validation (usually by gene knockout) in animal infection models (5). Until recently, this approach was limited to targets that are nonessential for bacterial growth in vitro because the corresponding mutants could not otherwise be generated for in vivo analysis. Thanks to the advent of inducible/repressible gene expression systems, it is now possible to construct conditional gene knockouts in mycobacteria. This powerful approach can be used to probe the role of the corresponding gene product at different stages of infection by delaying shutoff of the conditionally expressed gene (25). This is an important advantage because genes that are required for bacterial replication during the early stages of infection (acute phase) are not necessarily required for persistence at later stages (chronic phase).

Even this enhanced genetic approach to target validation has two potentially important shortcomings. First, functions that are dispensable for bacterial fitness in untreated animals could, in some cases, mediate bacterial persistence in treated animals because antimicrobials themselves have major effects on microbial physiology. These effects could sensitize or desensitize the bacteria to inhibition of other pathways. For example, it has been shown that antibiotics trigger a respiratory burst with concomitant generation of reactive oxygen species (ROS) (26). Thus, scavenging pathways for ROS detoxification could contribute to bacterial persistence in antibiotic-treated hosts even if the same pathways were dispensable in untreated hosts. Similarly, we found that disruption of *cydC* impaired *M. tuberculosis* persistence in INH-treated mice but did not affect bacterial growth/survival in untreated mice. Second, and conversely, functions that are important for bacterial fitness in untreated hosts might also, paradoxically, contribute to killing by conventional antimicrobials. For example, it has been shown that inhibition of bacterial respiration, which impairs energy metabolism and growth, can protect bacteria from antibiotic-mediated killing by preventing production of toxic ROS (26). Similarly, we found that transposon insertions within the *rv0096–rv0101* operon impaired *M. tuberculosis* growth and survival in untreated mice yet enhanced persistence in INH-treated mice.

The clinical relevance of persistence-impairing and persistence-enhancing mutations, as defined herein, is an important but as yet unaddressed issue. We note that a number of single-nucleotide polymorphisms of the *cydDC* and *rv0096–rv0101* loci are present in clinical *M. tuberculosis* isolates (http://www.tbdb.org). Although none of these mutations is predicted to eliminate or truncate the corresponding gene product, it is not unusual for missense mutations to cause loss or gain of function. The potential contribution of persistence-enhancing mutations to therapeutical failure would not be recognized by conventional diagnostic procedures because these mutations do not affect drug sensitivity of bacteria grown in vitro.

It is an attractive possibility that inhibitors targeting functions required for INH persistence might enhance the efficacy of conventional anti-TB regimens (which include INH), even if such inhibitors had no direct antimicrobial activity on their own. A clinically important example of this concept is provided by Augmentin, which comprises amoxicillin, a β-lactam antibiotic, and clavulanate, a β-lactamase inhibitor. On its own, clavulanate exhibits little or no antimicrobial activity, but it potentiates the activity of β-lactam antibiotics by preventing their degradation (27). The combination allows β-lactams to kill otherwise refractory bacteria, including *M. tuberculosis* (28). Similarly, compounds that inhibit the transcriptional repressor EthR enhance the activity of ethionamide against *M. tuberculosis* via increased expression of *ethA*, encoding a monooxygenase that activates ethionamide (29).

In *E. coli*, the ABC transporter encoded by *cydDC* is required for cytochrome *bd* oxidase assembly and maintenance of intracellular redox homeostasis (14). Transcriptional profiling of *M. tuberculosis* in mouse lungs revealed that progression from acute to chronic infection is accompanied by down-regulation of the low-affinity *aa3* type cytochrome *c*-oxidase and up-regulation of the high-affinity cytochrome *bd* oxidase (15). These observations suggest that disruption of *cydC* might impair intracellular redox homeostasis, thereby altering the cytoplasmic NADH/NAD$^+$ ratio. This is an intriguing possibility because INH is a prodrug that must be activated by covalent linkage to NAD, and it has been shown previously that mutations in *ndh*, encoding type II NADH dehydrogenase, cause INH resistance by increasing the NADH/NAD$^+$ ratio (30).

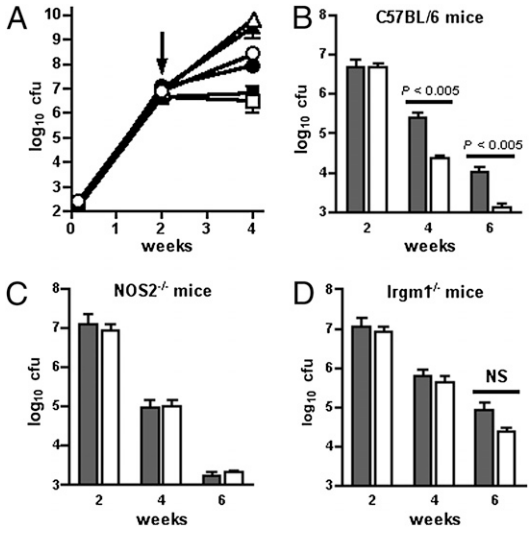

Fig. 4. Host immunity modulates INH-mediated killing of *cydC*::Tn bacteria. (*A–D*) Mice were infected by aerosol with ~200 cfus of WT (filled symbols and gray bars) or *cydC*::Tn (open symbols and white bars) bacteria. (*A*) Bacterial cfus were measured in the lungs of untreated C57BL/6 (■, □), NOS2$^{-/-}$ (●, ○), and Irgm1$^{-/-}$ (▲, △) mice at the indicated time points. Symbols represent mean ± SEM ($n = 4$). Groups of C57BL/6 (*B*), NOS2$^{-/-}$ (*C*), and Irgm1$^{-/-}$ (*D*) mice were treated with INH from 2 wk postinfection onward. Bacterial cfus were measured in the lungs at the indicated time points. Symbols represent mean ± SEM ($n = 4$). Results are representative of two experiments. Tukey's honestly significant difference test was used to compare the effectiveness of drug therapy (untreated vs. treated mice) against WT vs. mutant bacteria. *P* values are indicated for each time point where $P < 0.05$.

MICROBIOLOGY

However, *cydC* and *ndh* mutations should have similar effects on the NADH/NAD^+ ratio, yet these mutations have opposite effects on INH-mediated killing. It is possible that an as yet unknown CydC-dependent process other than redox homeostasis could account for the enhanced killing of *cydC* mutant bacteria by INH.

A recent study demonstrated that *E. coli* cytochrome *bd* oxidase is involved in resistance to nitric oxide because of its high kinetic off-rate (31). Because nitric oxide generated during the oxidative activation of INH by the *M. tuberculosis* catalase can inhibit bacterial respiratory enzymes (32), impaired cytochrome *bd* oxidase function might account for the enhanced INH-mediated killing of the *cydC*:: Tn mutant. However, this interpretation would not explain why this enhancement was observed only when the mutant bacteria were grown in vivo. Even conditions known to up-regulate *cydDC* expression, such as nitric oxide exposure or growth in IFN-γ–activated macrophages, have failed to reproduce the persistence defect of *cydC*::Tn bacteria in INH-treated mice. Future studies to uncover the mechanism whereby CydDC enhances INH-mediated killing would be greatly facilitated by the identification of in vitro conditions that reproduce the in vivo persistence defect caused by *cydC* disruption.

To avoid the aforementioned shortcomings of standard approaches to target identification and validation, drug discovery programs could incorporate strategies based on animal models of conventional drug therapy. Consistent with this notion, we have shown that this approach could identify targets that are essential for bacterial survival only in drug-treated animals. This category of potential targets would be overlooked by screening in untreated animals. Conversely, we have shown that this approach could avoid selection of targets whose inhibition would render the bacteria refractory to conventional drug therapy. Adoption of this approach might prevent costly late-stage failures in drug discovery.

Materials and Methods

Detailed methods are provided in *SI Materials and Methods*.

Bacteriology. *M. tuberculosis* strain Erdman and mutants were grown in Middlebrook 7H9 broth (Difco) containing 0.5% albumin, 0.085% NaCl, 0.2% glucose, 0.05% Tween-80, and 0.5% glycerol or on Middlebrook 7H10 agar (Difco) containing 10% OADC (Difco) and 0.5% glycerol. For drug susceptibility analysis, bacterial cultures (OD_{600} = 0.05) were exposed to INH (1.0 μg/mL) ± EMB (10 μg/mL) and aliquots were plated on 7H10 agar after washing with PBS containing 0.05% Tween-80.

Signature-Tagged Mutagenesis. Mutant library construction, genomic DNA isolation, signature tag amplification, and Southern blot hybridizations were as described (13). Hybridization signal intensities of individual signature-tagged mutagenesis tags were measured using an Amersham Biosciences Typhoon 9400 Imager.

Mouse Infections. Mice were infected by injection in a lateral tail vein with 5×10^6 cfus (inoculation of STM pools) or 1×10^6 cfus (monotypic retesting of mutants) or by aerosol with ~200 cfus of *M. tuberculosis* using a custom-built aerosol exposure chamber (19). Groups of mice were treated with INH (25 mg·kg·d), RIF (10 mg·kg·d), or PZA (150 mg·kg·d) delivered in the drinking water. Animal protocols were reviewed and approved by the chief veterinarian of the Swiss Federal Institute of Technology, by the Service de la Consommation et des Affaires Vétérinaires of the Canton of Vaud, and by the Swiss Office Vétérinaire Fédéral.

Statistical Analysis. Student's unpaired *t* test (two-tailed) was used for pairwise comparisons of WT vs. mutant strains of *M. tuberculosis*. Tukey's honestly significant difference test was used to compare the effectiveness of drug therapy (untreated vs. treated mice) against WT vs. mutant bacteria. $P < 0.05$ was considered significant.

ACKNOWLEDGMENTS. We thank James Gomez for assistance in the initial design and execution of the signature-tagged mutagenesis screen and Fred Ross and Jacques Rougemont for assistance with statistical analysis. N.D. was supported by a fellowship from the Charles E. Revson Foundation. This work was supported by a grant from the AstraZeneca Research Foundation and National Institutes of Health Grant 5 RO1 HL088906 (to J.D.M.).

1. Dye C, Lönnroth K, Jaramillo E, Williams BG, Raviglione M (2009) Trends in tuberculosis incidence and their determinants in 134 countries. *Bull World Health Organ* 87:683–691.
2. Ginsberg AM, Spigelman M (2007) Challenges in tuberculosis drug research and development. *Nat Med* 13:290–294.
3. van den Boogaard J, et al. (2009) Community vs. facility-based directly observed treatment for tuberculosis in Tanzania's Kilimanjaro Region. *Int J Tuberc Lung Dis* 13:1524–1529.
4. Young DB, Perkins MD, Duncan K, Barry CE, 3rd (2008) Confronting the scientific obstacles to global control of tuberculosis. *J Clin Invest* 118:1255–1265.
5. McKinney JD (2000) *In vivo veritas*: The search for TB drug targets goes live. *Nat Med* 6:1330–1333.
6. Rees RJ, Hart PD (1961) Analysis of the host-parasite equilibrium in chronic murine tuberculosis by total and viable bacillary counts. *Br J Exp Pathol* 42:83–88.
7. Muñoz-Elías EJ, et al. (2005) Replication dynamics of *Mycobacterium tuberculosis* in chronically infected mice. *Infect Immun* 73:546–551.
8. Gill WP, et al. (2009) A replication clock for *Mycobacterium tuberculosis*. *Nat Med* 15: 211–214.
9. McCune RM, Jr, McDermott W, Tompsett R (1956) The fate of *Mycobacterium tuberculosis* in mouse tissues as determined by the microbial enumeration technique. II. The conversion of tuberculous infection to the latent state by the administration of pyrazinamide and a companion drug. *J Exp Med* 104:763–802.
10. Jindani A, Aber VR, Edwards EA, Mitchison DA (1980) The early bactericidal activity of drugs in patients with pulmonary tuberculosis. *Am Rev Respir Dis* 121:939–949.
11. Camacho LR, Ensergueix D, Perez E, Gicquel B, Guilhot C (1999) Identification of a virulence gene cluster of *Mycobacterium tuberculosis* by signature-tagged transposon mutagenesis. *Mol Microbiol* 34:257–267.
12. Cox JS, Chen B, McNeil M, Jacobs WR, Jr (1999) Complex lipid determines tissue-specific replication of *Mycobacterium tuberculosis* in mice. *Nature* 402:79–83.
13. Hisert KB, et al. (2004) Identification of *Mycobacterium tuberculosis* counterimmune (*cim*) mutants in immunodeficient mice by differential screening. *Infect Immun* 72:5315–5321.
14. Cruz-Ramos H, Cook GM, Wu G, Cleeter MW, Poole RK (2004) Membrane topology and mutational analysis of *Escherichia coli* CydDC, an ABC-type cysteine exporter required for cytochrome assembly. *Microbiology* 150:3415–3427.
15. Shi L, et al. (2005) Changes in energy metabolism of *Mycobacterium tuberculosis* in mouse lung and under *in vitro* conditions affecting aerobic respiration. *Proc Natl Acad Sci USA* 102:15629–15634.
16. Parish T, Smith DA, Roberts G, Betts J, Stoker NG (2003) The *senX3-regX3* two-component regulatory system of *Mycobacterium tuberculosis* is required for virulence. *Microbiology* 149:1423–1435.
17. Rengarajan J, Bloom BR, Rubin EJ (2005) Genome-wide requirements for *Mycobacterium tuberculosis* adaptation and survival in macrophages. *Proc Natl Acad Sci USA* 102:8327–8332.
18. Wang F, Langley R, Gulten G, Wang L, Sacchettini JC (2007) Identification of a type III thioesterase reveals the function of an operon crucial for *Mtb* virulence. *Chem Biol* 14: 543–551.
19. MacMicking JD, Taylor GA, McKinney JD (2003) Immune control of tuberculosis by IFN-γ-inducible LRG-47. *Science* 302:654–659.
20. Feng CG, et al. (2004) Mice deficient in LRG-47 display increased susceptibility to mycobacterial infection associated with the induction of lymphopenia. *J Immunol* 172: 1163–1168.
21. MacMicking JD, et al. (1997) Identification of nitric oxide synthase as a protective locus against tuberculosis. *Proc Natl Acad Sci USA* 94:5243–5248.
22. Keating LA, et al. (2005) The pyruvate requirement of some members of the *Mycobacterium tuberculosis* complex is due to an inactive pyruvate kinase: Implications for *in vivo* growth. *Mol Microbiol* 56:163–174.
23. Muñoz-Elías EJ, Upton AM, Cherian J, McKinney JD (2006) Role of the methylcitrate cycle in *Mycobacterium tuberculosis* metabolism, intracellular growth, and virulence. *Mol Microbiol* 60:1109–1122.
24. Liu K, Yu J, Russell DG (2003) *pckA*-deficient *Mycobacterium bovis* BCG shows attenuated virulence in mice and in macrophages. *Microbiology* 149:1829–1835.
25. Gandotra S, Schnappinger D, Monteleone M, Hillen W, Ehrt S (2007) *In vivo* gene silencing identifies the *Mycobacterium tuberculosis* proteasome as essential for the bacteria to persist in mice. *Nat Med* 13:1515–1520.
26. Dwyer DJ, Kohanski MA, Collins JJ (2009) Role of reactive oxygen species in antibiotic action and resistance. *Curr Opin Microbiol* 12:482–489.
27. Bush K (1988) Beta-lactamase inhibitors from laboratory to clinic. *Clin Microbiol Rev* 1: 109–123.
28. Hugonnet JE, Tremblay LW, Boshoff HI, Barry CE, 3rd, Blanchard JS (2009) Meropenem-clavulanate is effective against extensively drug-resistant *Mycobacterium tuberculosis*. *Science* 323:1215–1218.
29. Willand N, et al. (2009) Synthetic EthR inhibitors boost antituberculous activity of ethionamide. *Nat Med* 15:537–544.
30. Vilchèze C, et al. (2005) Altered NADH/NAD+ ratio mediates coresistance to isoniazid and ethionamide in mycobacteria. *Antimicrob Agents Chemother* 49:708–720.
31. Mason MG, et al. (2009) Cytochrome *bd* confers nitric oxide resistance to *Escherichia coli*. *Nat Chem Biol* 5:94–96.
32. Timmins GS, Master S, Rusnak F, Deretic V (2004) Requirements for nitric oxide generation from isoniazid activation *in vitro* and inhibition of mycobacterial respiration *in vivo*. *J Bacteriol* 186:5427–5431.